A New Chemical Sensing Material for Ethanol Detection: Graphene-Like Film

B. Alfano[1,2(✉)], M. Alfè[3], V. Gargiulo[3], T. Polichetti[1], E. Massera[1], M.L. Miglietta[1], and G. Di Francia[1]

[1] ENEA C.R. Portici, P.le E. Fermi 1, 80055 Portici, Naples, Italy
brigida.alfano@enea.it
[2] Department of Physical Sciences, University of Naples Federico II, via Cinthia, 80126 Naples, Italy
[3] Institute for Research on Combustion (IRC)—CNR, p.le V. Tecchio 80, 80125 Naples, Italy

Abstract. The development of volatile organic compounds (VOCs) sensor, operating at room temperature (RT), is a challenge for the research community. In this framework, we present a device based on a graphene-like (GL) material suitably tested as sensing layer for the ethanol detection. GL material was obtained through a two steps oxidation/reduction method starting from a nanostructured carbon black. GL material combines a defect-free basal plane graphenic structure with the presence of oxygen functional groups, mainly carboxylic, located on the layer edges. A GL-based device was realized and investigated for the detection of ethanol. The experiments were performed under atmospheric pressure, in a dry air and at RT. Results showed that GL material is a promising candidate for the detection of low concentration of ethanol at RT.

Keywords: Graphene-like materials · Oxidized carbon black · Gas sensors · VOCs detection · Ethanol sensing device · Room-temperature device

1 Introduction

Metal-oxide semiconductors are widely used as sensing layers for the detection of VOCs, due to their high sensitivity, fast response, recovery and stability. However, one major drawback of this type of sensors is the high temperatures required for their operation (200–450 °C) [1–3] and the consequent high power consumption. Although the introduction of nanocrystals and nanowires have improved the sensing performances and lowered the operating temperatures of metal oxides based sensors [4–6] in the last years, also other materials have been considered for the development of new gas sensors. Carbon-based nanomaterials proved to be promising for this scope due to their intrinsic electrical properties, high surface area, high chemical and thermal stability and functionalization capability [7]. Among the large family of carbon-based nanomaterials, graphene and graphene related materials (GRMs) in the last years have been explored for the detection of a widespread range of chemicals, including VOCs [8].

Graphene-like (GL) layers are carbon-based nanomaterials obtained through a two steps oxidation/reduction method starting from a carbon black (CB) [9, 10], consisting in small graphenic flakes (about four graphenic layers of thickness) decorated at the layer edge with oxygen functional groups (mainly carboxylic/carbonylic). Differently from graphite oxide (GO), in GL material the basal planes of the graphitic network are preserved from defect, which represents a clear advantage for the conductivity and the electronic properties. GL layers in aqueous suspension are a versatile material as testified by its use in the preparation of a large variety of hybrid materials. When intercalated in insulating Metal-Organic Frameworks (MOFs), GL layers allow to produce composites with tunable electrical conductivity [11]; when combined with Eumelanin by a copolymerization approach, GL layers produced a biocompatible interface with conductive and adhesive properties very promising for biosensoristic applications [12] and when covered by TiO_2-nanoparticles by a co-precipitation strategy GL layers produced a material with improved photocatalytic activities [13].

In this framework, we have realized a prototypal chemiresistive sensing device for ethanol detection based on GL film. The device was tested under atmospheric pressure, in dry air and at RT. The results showed that GL material is a promising candidate for the detection of low concentration of ethanol at RT.

2 Experimental

2.1 Realization of the Prototypal Chemiresistive Sensing Device

Analytical grade chemicals were purchased from Sigma Aldrich and used as received. CB (furnace black, N110 type, 15–20 nm primary particle diameter, specific BET area 139 m^2/g) was obtained by Sid Richardson Carbon Co.

GL layers in aqueous suspension were produced from a nanostructured CB following a synthetic approach that consists in an oxidation step followed by a chemical reduction with hydrazine. A detailed description of the synthetic procedure is reported elsewhere [9, 10]. Briefly: 500 mg of CB were oxidized for 90 h with 10 mL of HNO_3 (67 wt%) at 100 °C under reflux and stirring. The oxidized material was recovered by centrifugation and washed many times with distilled water in order to remove any acid traces. After the oxidation step 60 mg of oxidized material were dispersed in 60 mL of distilled water and treated with 1.35 mL of hydrazine hydrate (50%) for 24 h at 100 °C under reflux. The excess of hydrazine was neutralized with nitric acid (4 M) allowing the precipitation of a black solid (GL layers). GL layers were recovered by centrifugation and washed two times with distilled water in order to remove salts and acid traces. The GL layers were stored as aqueous suspension at 1 mg/L of concentration and pH 3.7.

GL film was obtained by drop-casting the GL water dispersion onto transducers and dried at RT, realizing a prototypal chemiresistive device. The transducers employed for the electrical and sensing characterization of the GL films, have 5 pairs of gold interdigitated electrodes (IDEs) electrodeposited onto rough alumina substrate: each electrode finger is 350 μm wide and 4650 μm long. The spacing between fingers is 350 μm.

2.2   Characterization Equipment

X-ray photoemission spectroscopy (XPS) was performed in a ultra-high vacuum chamber (base pressure of 1×10^{-10} mbar) equipped with a Specs Phoibos 150 electron analyzer, using Al K_α (photon energy: 1486.6 eV) X- ray source.

GL aqueous suspensions (100 µL of a 1 mg/mL GL suspension) were drop-casted onto the device, allowed to dry in air at ambient temperature and analyzed by atomic force microscopy (AFM). The AFM images were acquired on a XE100 Park instrument operating in noncontact mode (amplitude modulation, silicon nitride cantilever from Nanosensor) at room temperature and in ambient conditions.

The ethanol for gas-sensing characterizations comes from certified cylinder containing calibrated vapour balanced in dry air at 100 ppm (Ossi gas srl). The gas flow mixing rates were precisely and rapidly manipulated using computer mass flow controllers (MKS) and electro-pneumatic valves. A bias voltage fixed at 1 V was applied to the electrodes with a Precision Power Supply TTi QL355T and the conductance values were registered using a high resolution picoammeter Keithley 6485.

The gas-sensing performances of the sensing device were characterized towards ethanol under atmospheric conditions (24 ± 2 °C and 1.00 ± 0.05 bar) in a sealed stainless steel chamber. A constant flux of synthetic dry air of 500 sccm as gas carrier was flowed and mix with the desired concentration of ethanol. After 30 min in dry air (baseline), the sensing device was exposed to the analyte concentration for 30 min and the air flux was then restored for 60 min. The percentage response (S) is defined as the maximum of the conductance variation reached by the device during the analyte exposure that is $[|G - G_0|/G_0] \times 100$, where G and G_0 are the conductance recorded during analyte exposure and baseline acquisition steps, respectively.

3   Results and Discussion

GL film was prepared as described in the Experimental section. A detailed characterization of the material was reported in [9, 10] and here summarized for sake of clarity. The synthesis procedure allow high yields (55 wt% of recovery) of GL layers with a multi-layered graphenic structure (about four layers) characterized by a preserved graphitic network, i.e. with functionalization only at the borders of the graphenic layers [9, 10]. The H/C atomic ratio is 0.32 and the O/C atomic ratio: 0.56. The functionalization consists of residual oxygen functional groups, mainly carboxylic groups (pKa 3.4, number of sites 900 mmol/g). Lactones and anhydrides are also present (pKa 5.5, number of sites 240 mmol/g). The oxygen functional groups allow establishing a zeta potential around −30 mV at pH 2 and around −45 mV at pH 12 [10].

Characterization by X-ray Photoemission Spectroscopy (XPS) on powders and imaging by Atomic Force Microscopy are reported in the following.

XPS spectrum is reported in Fig. 1 along with its deconvolution into Gaussian components after Shirley background subtraction using a home-made software.

C1s XPS spectrum on GL sample and its deconvolution in Gaussian shape peaks demonstrate the presence of different oxygen functional groups. In particular, there are
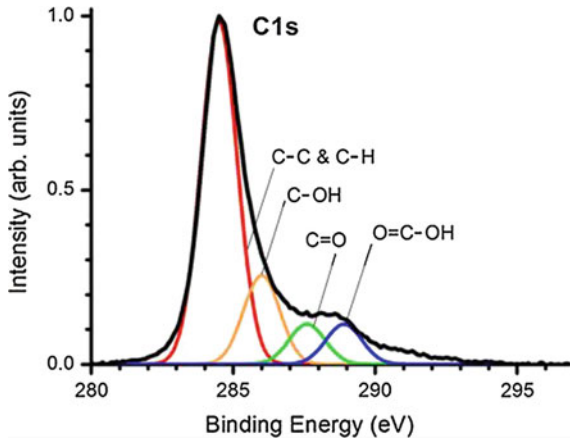
Fig. 1. C1s XPS spectrum on GL film, and its deconvolution in Gaussian shape peaks corresponding to different functional groups (modified from [10])

four components located at 284.5 eV (carbon involved in C=C and C–H bonding), 286 eV (C–OH), 287.5 eV (C=O), 289 eV (COOH).

AFM morphological characterization on a film obtained on mica substrate by drying in air a drop-casted GL layers suspension (pH 3.7, 1 mg/mL) provided an estimation of the surface roughness, as shown in Fig. 2.

AFM topographic image shows a flat morphology over a large area (5 × 5 μm). The roughness, estimated by the scan profile (Fig. 2b) is about 0.1 nm peak to peak over a distance of 3 μm. This value clearly indicate flatness at atomic level, characteristic of the GL layers allowed to self-assembly on a flat surface from suspension at pH 3.7 [10].

I–V measurements performed on GL film showed linear behavior (Fig. 3a), which implies an Ohmic contact between GL sheets and gold electrodes. Figure 3b displays the dynamic response of the device exposed to 50 ppm of ethanol at RT in dry air. GL material is responsive to ethanol, exhibiting a conductance variation equal to 3% (Fig. 3b). This result is even more astonishing when compared to the detection limits of other devices operating at RT reported in the literature [15], including pristine graphene which results as totally insensitive to ethanol.

Employing the mathematical model shown in our previous work [16], it is possible calibrate the device correlating directly the time derivative of the device conductance to the interacting analyte concentration. In particular, defining the reactivity as the maximum of the device conductance rate, it is possible to correlate the reactivity to the analyte concentration. Besides, reaction time is here defined as the time in which the aforementioned maximum of the conductance rate is reached; by extension, the reaction time can be regarded as the time taken by the device to detect a given analyte concentration. The exposure to several sequential steps at different analyte concentrations (black solid squares in Fig. 4), ranging from 0 ppm down to 100 ppm, discloses a linear correlation between the device reactivity and the analyte concentration.
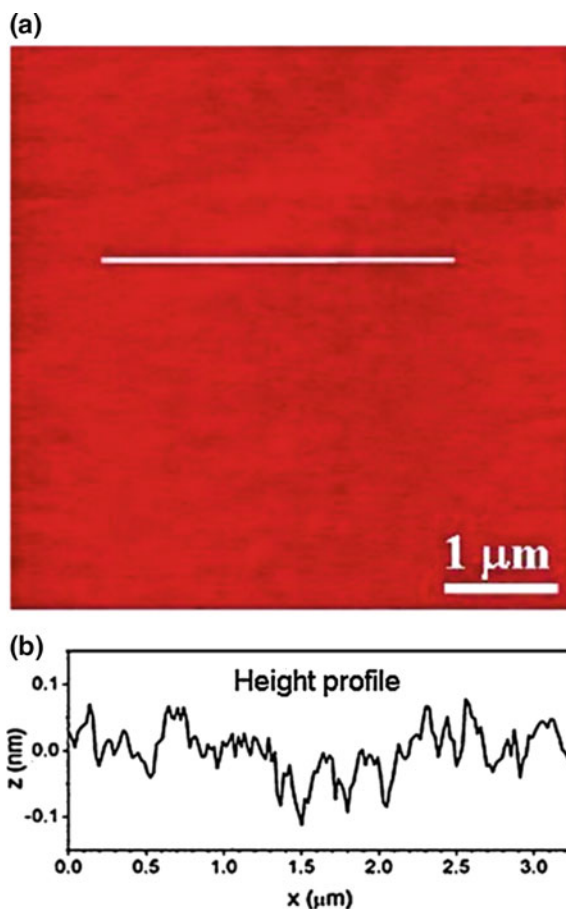
(a)

1 μm

(b)

Height profile

z (nm)

0.1

0.0

-0.1

0.0   0.5   1.0   1.5   2.0   2.5   3.0

x (μm)

Fig. 2. AFM topographic image (scan area 5 μm × 5 μm, **a**) with a line profile (**b**) (modified from [10])

The black solid squares represent the data of the maxima of the device conductance rate corresponding to different concentrations. The red straight line represents the best fit for the collected data. Taking into account the error bars, it can be evaluated that the limit of detection (LOD) for this device is around 10 ppm.

The device reaction time shows a non-linear relation with the analyte concentration (blue squares in Fig. 4). For concentrations in the range 40–100 ppm the device responds in about 40 s while in the low concentration range, i.e. from 10 to 20 ppm, a clear increase of the reaction time is observed. Nevertheless, the device takes less than 60 s to detect 20 ppm of ethanol.
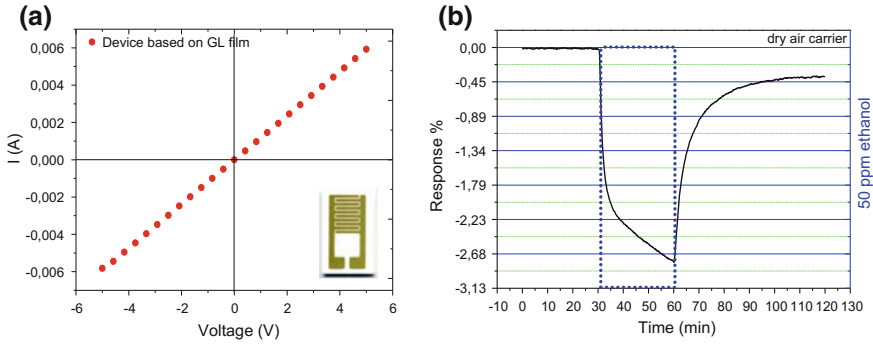
Fig. 3. Electrical characterizations: **a** typical I–V curves of device based on GL film. Data were collected in the range [−5, 5 V], in the inset, an image of the transducer; **b** response to 50 ppm of ethanol in dry air using a GL based sensor
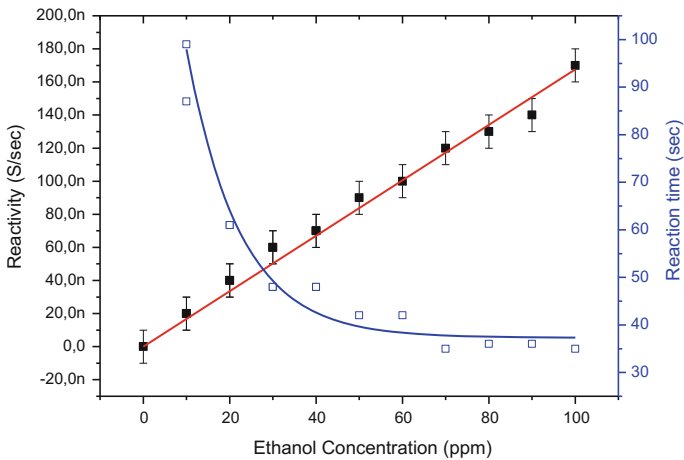

Fig. 4. Ethanol-sensing calibration at RT of the GL film based device in the range 0–100 ppm in dry air carrier. The *red straight line* fits the points of maximum of the conductance rate (reactivity) collected at different ethanol concentrations. Reaction times are plotted versus ethanol concentration (*blue squares*) (Color figure online)

4   Conclusions

We have realized a prototypal chemiresistive sensing device for ethanol detection based on GL film obtained by the self-assembly of GL layers, a carbon-based nanomaterial consisting in small graphenic flakes obtained through a two steps oxidation/reduction method starting from a nanostructured carbon black. The prototypal device was tested under atmospheric pressure, in dry air and at RT and exhibiting a conductance variation equal to 3% to low ethanol concentration (50 ppm). The LOD results around 10 ppm. This result showed that GL material is a promising candidate for the detection of low concentration of ethanol at RT.

References

1. A. Umar, J.-H. Lee, R. Kumar, O.A. Dossary, A.A. Ibrahim, S. Baskoutas, Mat. Des. **105**, 16–24 (2016)
2. C.C. Yang, X. Su, F. Xiao, J. Jian, J. Wang, Sens. Actuators B **158**, 299–303 (2011)
3. N. Hongsith, C. Viriyaworasakul, P. Mangkorntong, N. Mangkorntong, S. Choopun, Ceram. Int. **34**, 826–834 (2008)
4. G. Neri et al., Sens. Actuators B **130**, 222–230 (2008)
5. J.M. Wu. Nanotechnol. **21**, 235501 (6 pp) (2010)
6. M. Mabrook, P. Hawkins, Sens. Actuators B Chem. **75**, 197–202 (2001)
7. E. Llobet, Sens. Actuators B **179**, 32–45 (2013)
8. S.S. Varghese, S. Lonkar, K.K. Singh, S. Swaminathan, A. Abdala. Sens. Actuators B **218**, 160–183 (2015)
9. F. Schedin, A.K. Geim, S.V. Morozov, E.W. Hill, P. Blake, M.I. Katsnelson, K.S. Novoselov. Nat. Mater. 6652–655 (2007)
10. M. Alfè, V. Gargiulo, R. Di Capua, F. Chiarella, J.-N. Rouzaud, A. Vergara, Anna Ciajolo, ACS Appl. Mater. Interfaces **4**, 4491–4498 (2012)
11. M. Alfè, V. Gargiulo, R. Di Capua, Appl. Surf. Sci. **353**, 628–635 (2015)
12. M. Alfè, V. Gargiulo, L. Lisi, R. Di Capua, Mater. Chem. Phys. **147**(3), 744–750 (2014)
13. V. Gargiulo, M. Alfè, R. Di Capua, A.R. Togna, V. Cammisotto, S. Fiorito, A. Musto, A. Navarra, S. Parisi, A. Pezzella, J. Mater. Chem. B **3**, 5070 (2015)
14. M. Alfè, D. Spasiano, V. Gargiulo, G. Vitiello, R. Di Capua, R. Marotta, Appl. Catal. A Genl. **487**, 91–99 (2014)
15. T. Wang, D. Huang, Z. Yang, S. Xu, G. He, X. Li, L. Zhang, Nano-Micro Lett. **8**, 95–119 (2016)
16. F. Ricciardella, E. Massera, T. Polichetti, M.L. Miglietta, G. Di Francia, Appl. Phys. Lett. **104**(18), 183502 (2014)